CONTRACT SERIAL NO. 99182-01-SQ
CONTRACT REQUISITION NO. 23440-9-9182
CONTRACTOR: UNIVERSITY OF SHERBROOKE

PROJET No. 9-9182

MICROSTRUCTURAL DEVELOPMENT IN ALKALI ACTIVATED SLAG CONCRETE

by

Dr. Shondeep L. Sarkar and

Dr. Arezki Tagnit-Hamou

Faculté des sciences appliquées
Université de Sherbrooke
Sherbrooke, Québec

Final report submitted to

Dr. Esther Douglas
CANMET, Ottawa

MICROMEDIA

46 pp

October 1990

INTRODUCTION

This report is a follow-up of the previous one entitled "Microstructural development in (i) lime and (ii) alkali activated slag", submitted in July 1990. In this part of the project, attention was focussed on the study of the microstructure of slag activated concrete at 1d, 7d, 28d, and 91 days.

The concrete samples prepared and acetone dried at CANMET were supplied to the reporters for microstructural investigation by means of SEM/EDXA and XRDA.

CONCRETE COMPOSITION

The concrete composition given in Table 1 shows that MS (1.47) used for making the concrete is slightly higher than that of the paste (1.36) - vide previous report.

TABLE 1

Composition of alkali activated slag concrete

Material	Weight
Water	271
Slag, kg/m^3	454
Coarse aggregate, kg/m^3	1808
Fine aggregate, kg/m^3	1421
Water glass, L/m^3	217
Lime slurry, L/m^3	40
AEA, L/m^3	18
W/B	0.50

Na_2SiO_3/slag = 0.48

Na_2SiO_3/lime = 11.0

MS = 1.47

Air content = 3.6%

CONCRETE STRENGTH

Table 2 below shows the compressive strength to be high at 1d. A significant rise in strength occurs between 1 and 7d. Similar trend is noticed between 28 and 91 d.

TABLE 2

Compressive strength of AAS concrete (MPa)

1d	7d	28d	91d
26.9	39.2	43.4	51.6

MICROSTRUCTURAL DEVELOPMENT: SEM EXAMINATION

Day 1: The paste-aggregate bonding at Day 1 has not developed properly. This is manifested by the presence of cracks and fissures representing debonding in the transition zone. The width of these cracks varies from < 1 μm to 5 μm (figs. 1-3). Some unreacted slag grains are visible in the transition zone (figs. 2 and 3). The composition of the surrounding gel in this region (fig. 4) shows there is very little incorporation of Mg, Al and Na in the gel. This is evident when one compares the composition of a partly reacted slag grain (fig. 5) which has higher Mg and Al in it. Even when partially reacted slag grains as in fig. 6 are present in the transition zone, the bonding between the paste and the aggregate appears to be rather weak.

The paste composed of an already densified gel exhibits numerous irregular fissures (fig. 7).

The mottled appearance of this gel in certain parts is due to localized lime enrichment. This is clear from the EDX spectra (figs. 8 and 9), the former representing the composition of the smooth part of the gel, and the latter with higher Ca is the mottled region. A very small amount of Na incorporation in the gel is also detectable.

In general, however, the gel has a smooth external appearance (fig. 10).

An important observation is the presence of intact slag grains with relatively smooth surfaces (figs. 11 and 12) enveloped in a dense but cracked gel. This feature is a significant departure from the normal hydrated slag which develops accicular growth on the surface during hydration. The slag particles at this stage of hydration do not show any signs of internal cracking.

Microstructure of AAS concrete at 1 day

Fig. 1. A fine fissure in the transition zone. Aggregate-right, paste-left

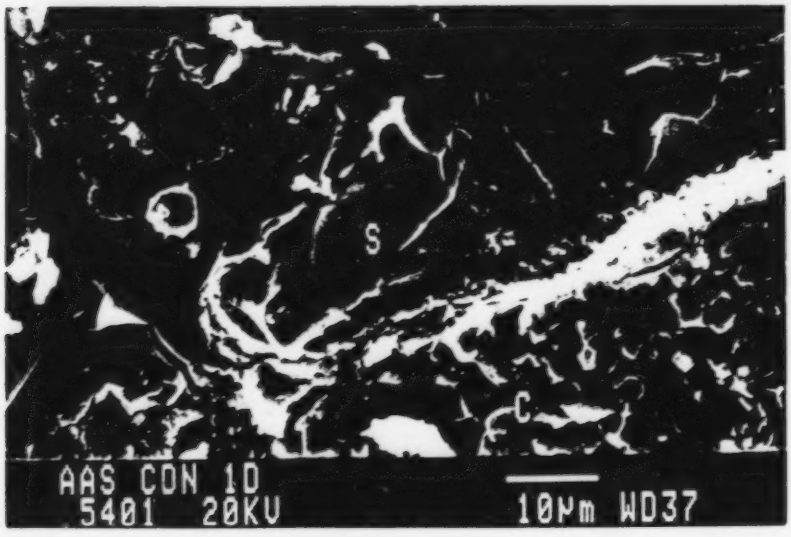

Fig. 2. Wider fissure in the transition zone. S-slag particle

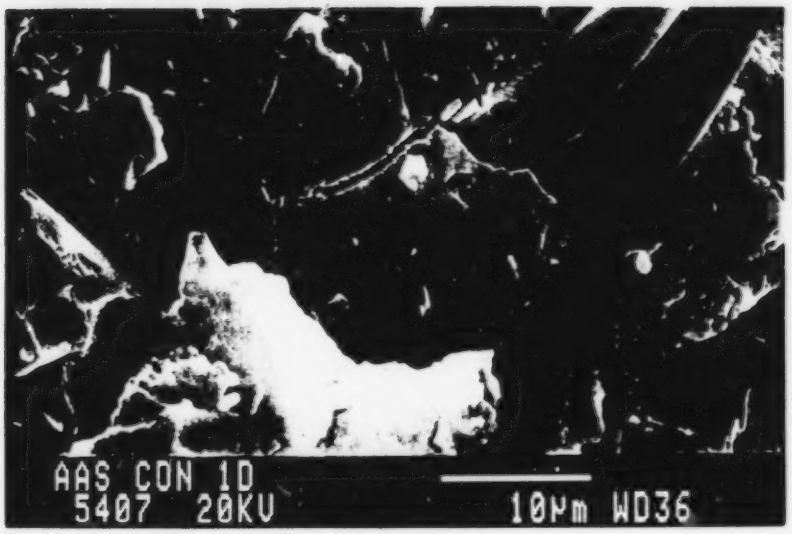

Fig. 3. Maximum gap of 5 µm between paste and aggregate. The smooth particles are slag. Aggregate-right, paste-left

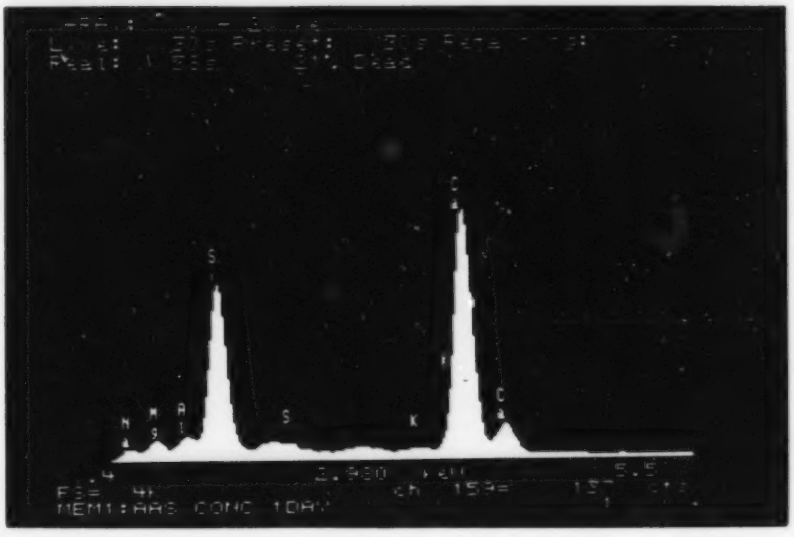

Fig. 4. Composition of the adjacent gel

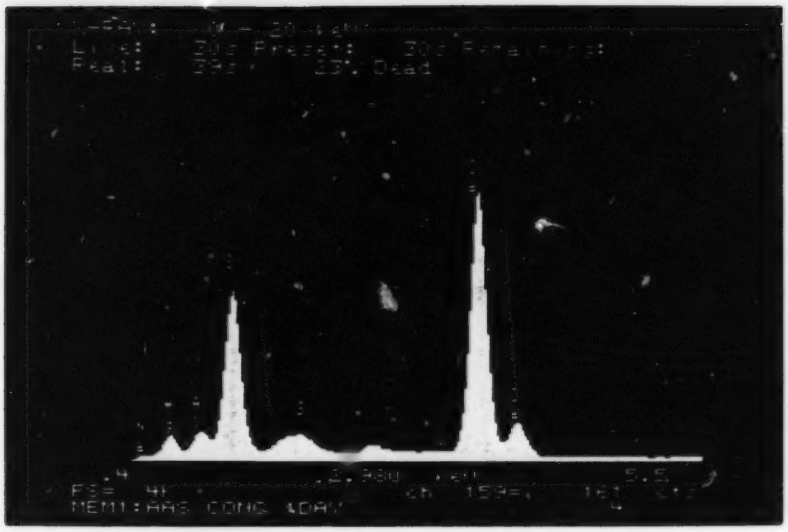

Fig. 5. Composition of partly reacted slag in the transition zone

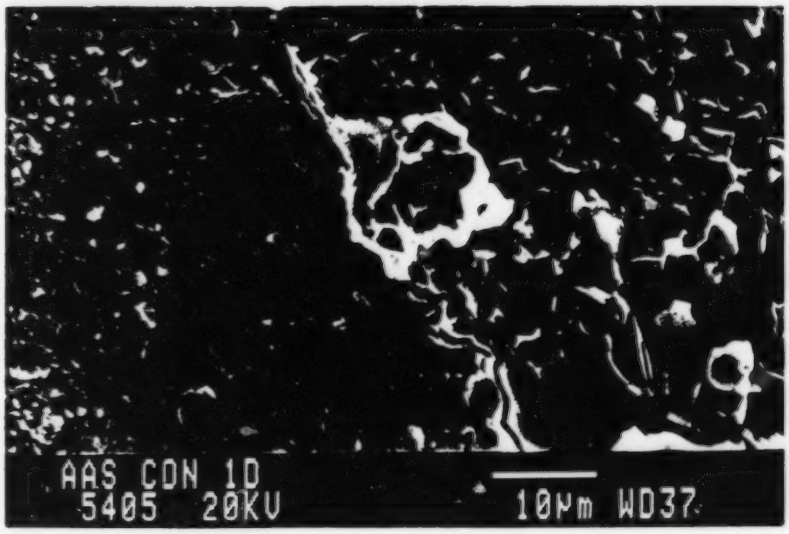

Fig. 6. View of this slag particle. Fissure is still present in the transition zone. Aggregate-right

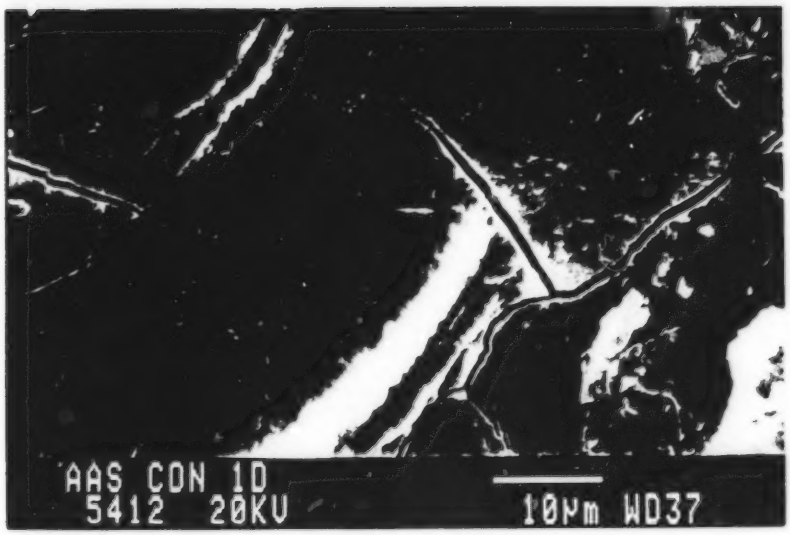

Fig. 7. Dense gel with several cracks in it. Mottling is due to localized lime enrichment

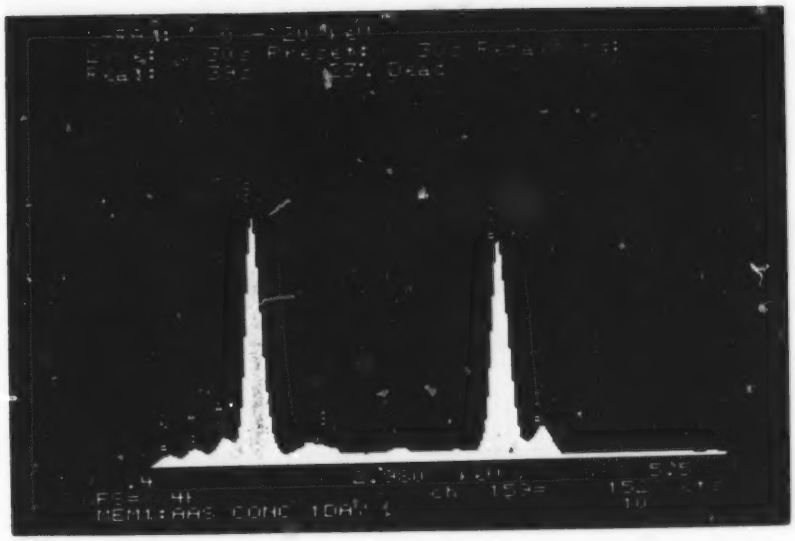

Fig. 8. Composition of smooth part of this gel

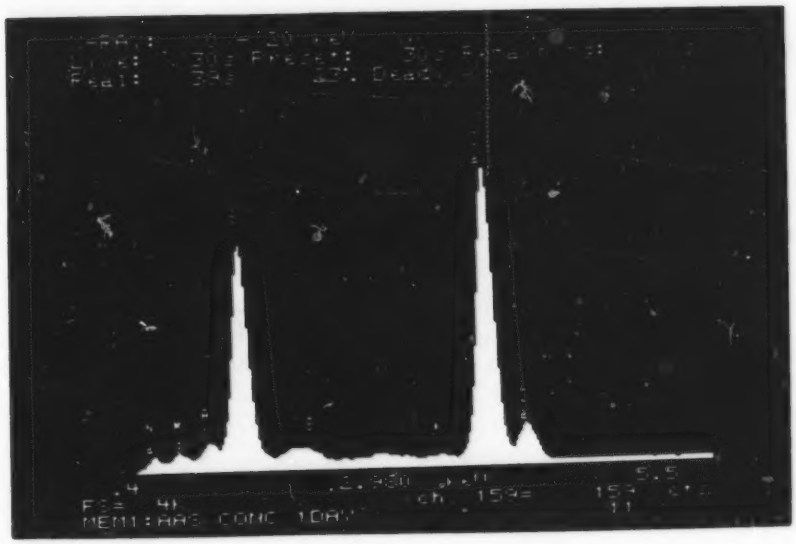

Fig. 9. Composition of the mottled part showing higher Ca

Fig. 10. Smooth surface of gel

Fig. 11. An unreacted slag with smooth surface in the paste

Fig. 12. Another slag particle showing the same feature

Day 7: There is no improvement in the paste-aggregate bonding. Fine-to-wide fissures (up to 5 μm) are distinctly visible in the transition zone (figs. 13-15).

The paste in the interfacial zone shows abundant cracks (figs. 16 and 17). The composition of this gel, however, is the same (fig. 18), as the paste gel, a small amount of Na, Mg and Al being present.

Though slag with smooth intact surfaces are present (figs. 19 and 20), internal cracking has commenced in a number of grains (fig. 21). These cracked grains, however, still retain their external smoothness. Some of these grains, despite their surface smoothness, appear to develop a thin reaction rim (figs. 22 and 23). The size of the grain does not seem to affect the formation of the rim.

The gel in the matrix is dense, but cracked (fig. 24) as at Day 1. The composition of the matrix gel is the same, except for slight variation in the Mg content, indicating dissolution of slag in places where the Mg is higher (figs. 25 and 26).

Microstructure of AAS concrete at 7 days

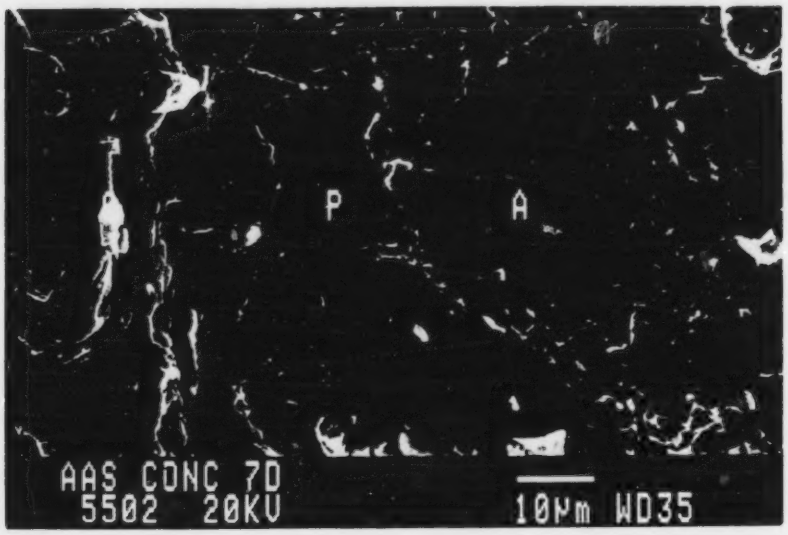

Fig. 13. Fine fissure along the paste-aggregate boundary. A- aggregate, P- paste

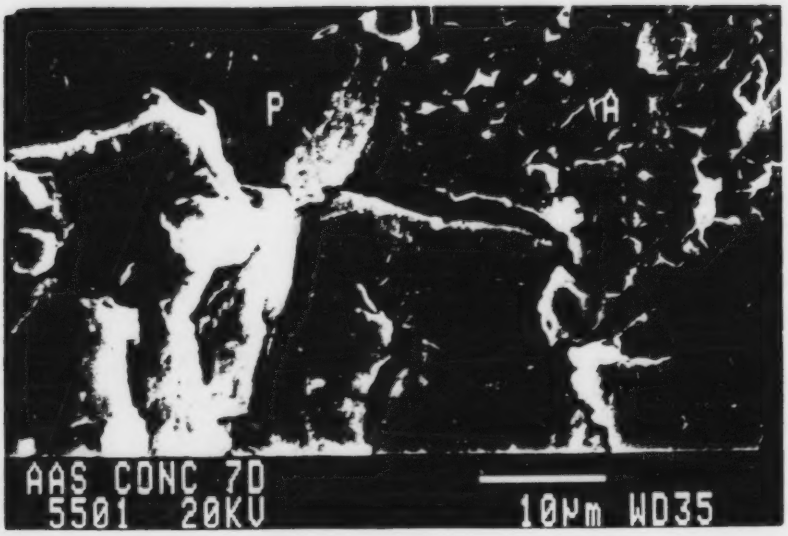

Fig. 14. Slightly enlarged fissure in the transition zone. A- aggregate, P- paste

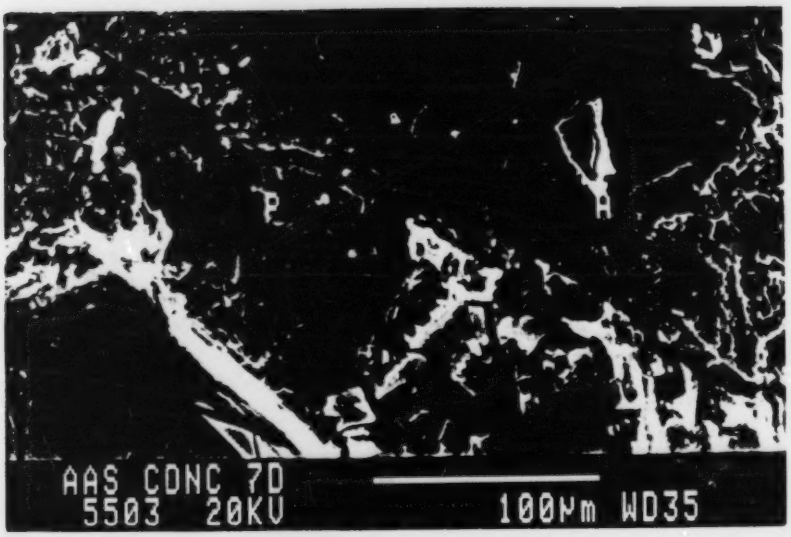

Fig. 15. Wide fissure in the transition zone

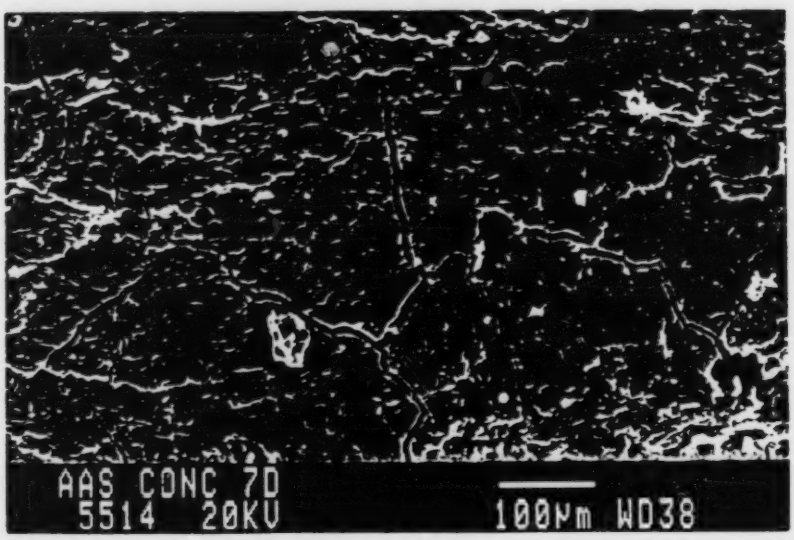

Fig. 16. Showing cracks in the paste of the interfacial zone

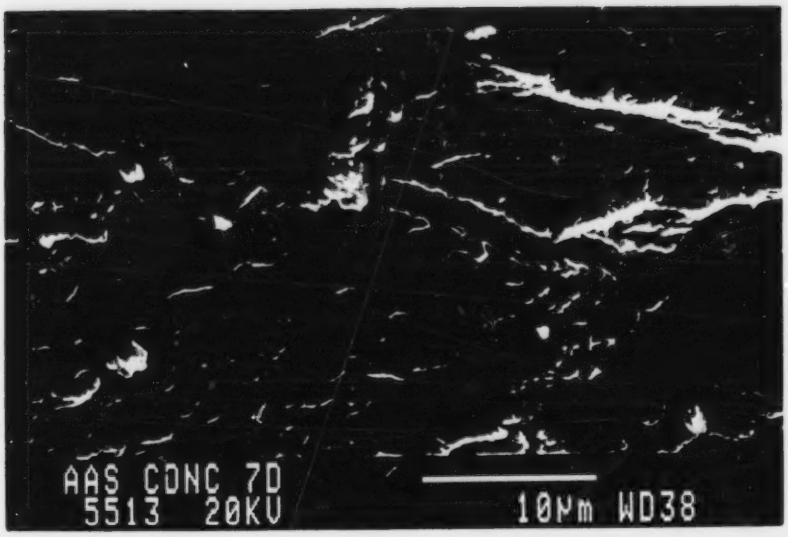

Fig. 17. Magnified view of this zone

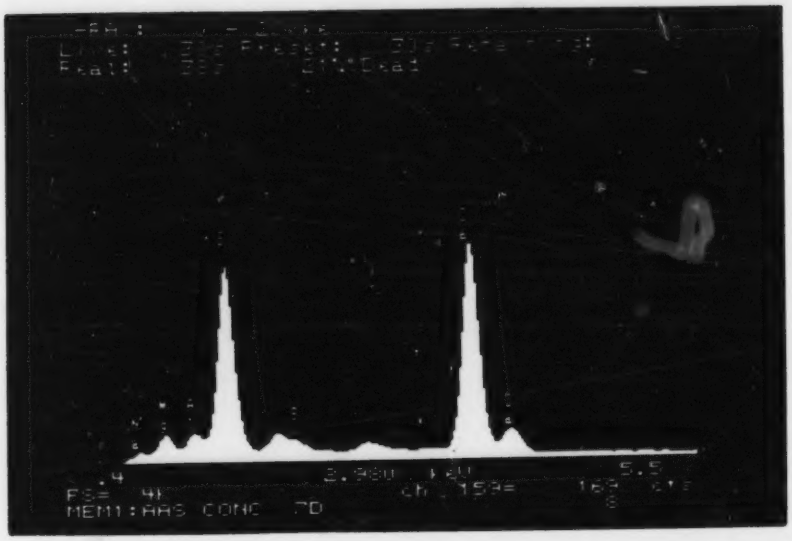

Fig. 18. Composition of the paste in this zone

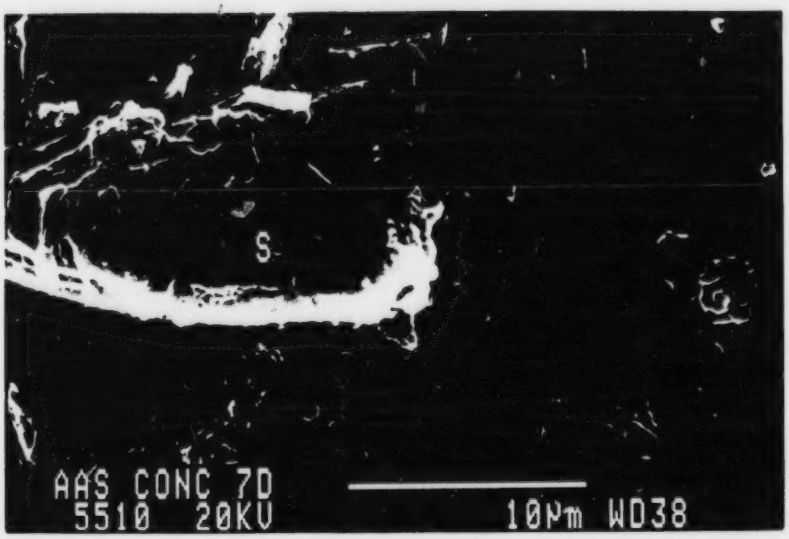

Fig. 19. Smooth intact slag grain in the paste

Fig. 20. Another such grain in the paste

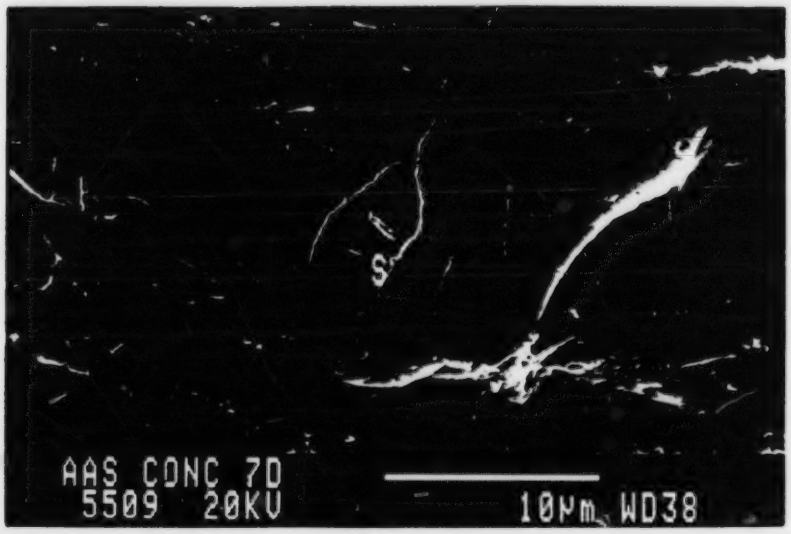

Fig. 21. Internal cracking in a slag grain

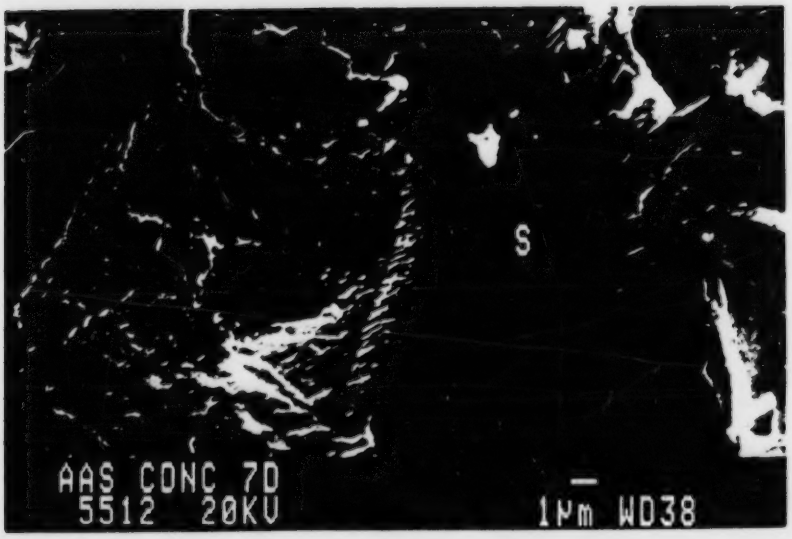

Fig. 22. A thin reaction rim around a large smooth slag grain

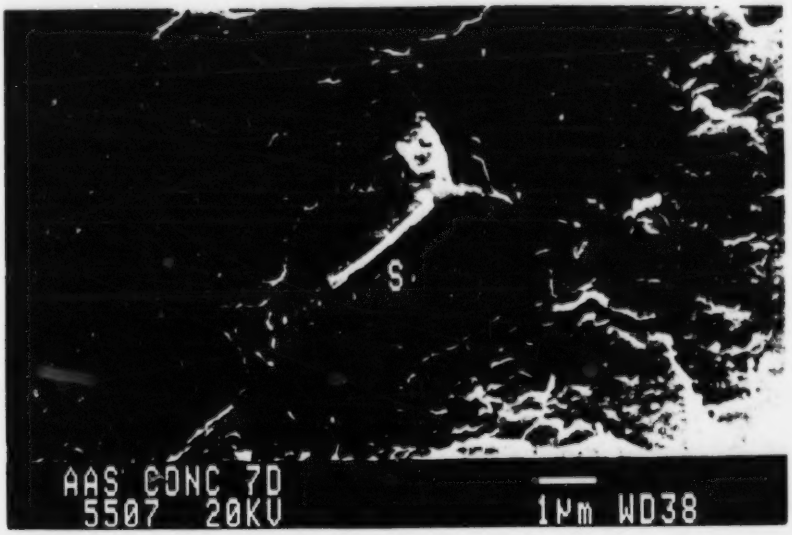

Fig. 23. A thin reaction around a much smaller smooth slag grain surrounded by dense gel

Fig. 24. Dense but cracked gel in the paste

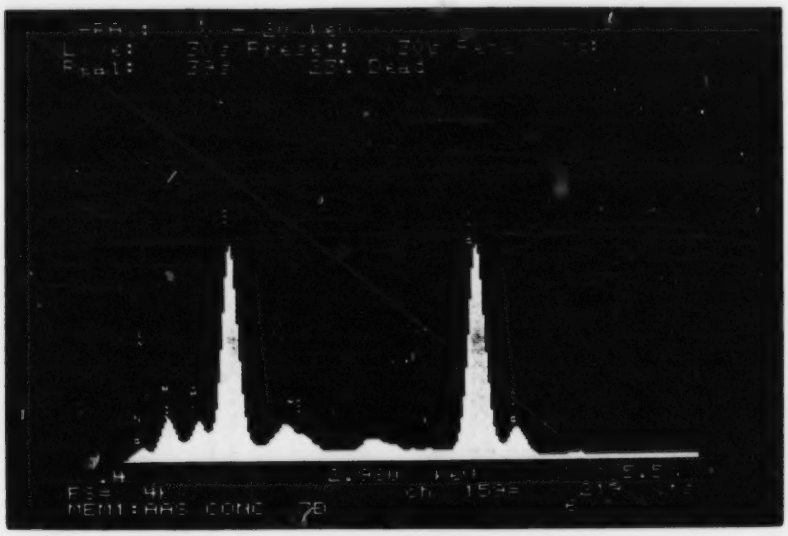

Fig. 25. Composition of paste gel showing higher Mg due to slag dissolution

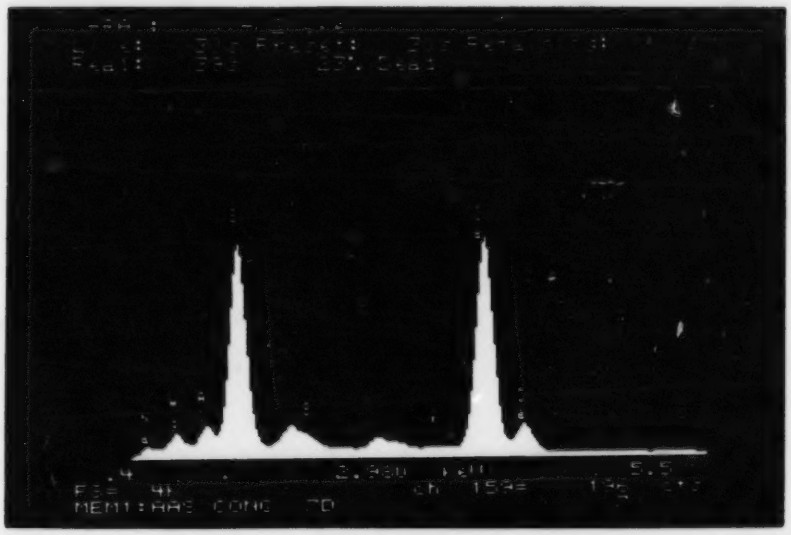

Fig. 26. Composition of paste gel with lower Mg content

Day 28: The paste aggregate bonding has become much stronger (figs. 27-28). The smooth region in Figure 27 can be identified as slag (fig. 29) because of its higher Mg, whereas the gel around it shows lower Mg content (fig. 30). Some parts (fig. 31) show an increase in the amount of Na (fig. 32).

The interfacial zone exhibits an entirely different microstructure at 28 days (fig. 33), though its composition is virtually the same (fig. 34). A strong concentration of Na was found in certain parts of the interfacial zone of this particular sample. A semipermeable membrane enriched in Na has developed (figs. 35-37). Though the Na content of this layer is appreciably lower in some locations (fig. 38), it is by far the highest amount recorded among all the samples. Apart from this membranous structure, tiny globules (< 1 μm dia.), often linked together, are present (figs. 39-41). These globules also exhibit a high concentration of Na (fig. 42). It appears as though the semipermeable membrane is constituted of a large number of these tiny globules.

The paste gel shows no reduction in cracks (figs. 43 and 44). Its appearance is identical to that of 1d and 7 days, ie, smooth and compact but cracked. Its composition is also similar (fig. 45), with occasional increase in Mg, the quantity of Mg representing slag dissolution. Smooth intact grains of slag (fig. 46) as well as cracked grains (figs. 47 and 48) persist in the paste. One observes that the cracking phenomenon is independent of the size of the grain. Both relatively small, as well as large grains exhibit identical cracking. These grains are intimately associated with the surrounding gel. In the case of the smooth grains, some peripheral reaction is apparent.

Microstructure of AAS concrete at 28 days

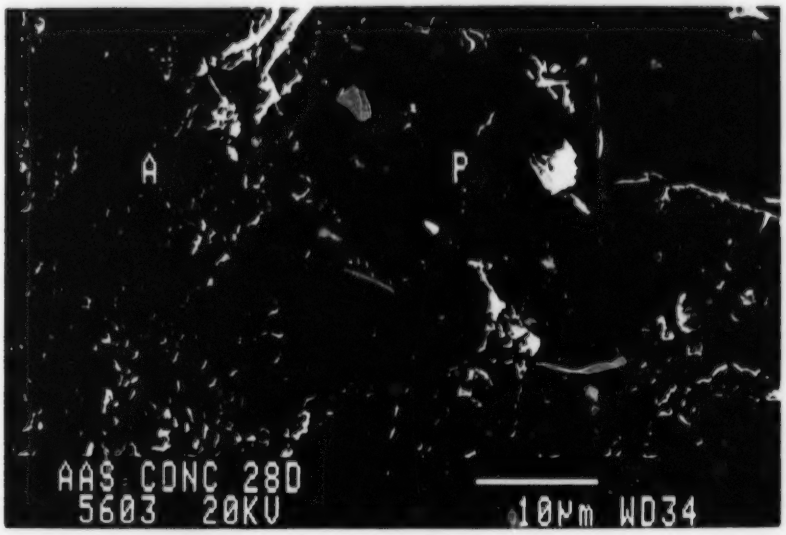

Fig. 27. Strong paste-aggregate bonding. A- aggregate, P- paste. The smooth particle is a slag grain, and the rest forms the gel

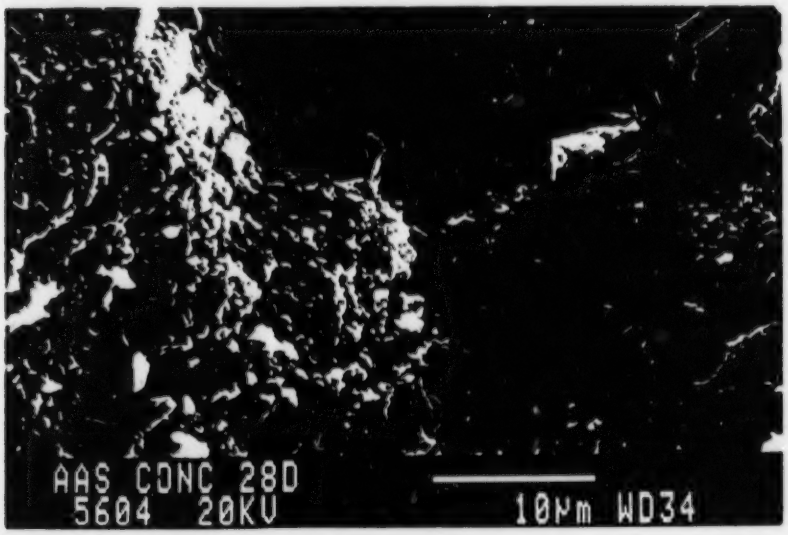

Fig. 28. Same feature, another area

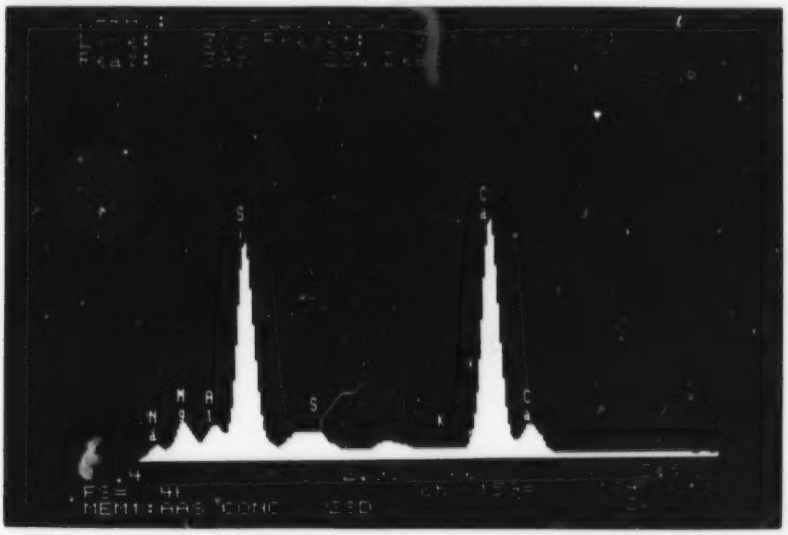

Fig. 29. Composition of the slag grain shown in Figure 27

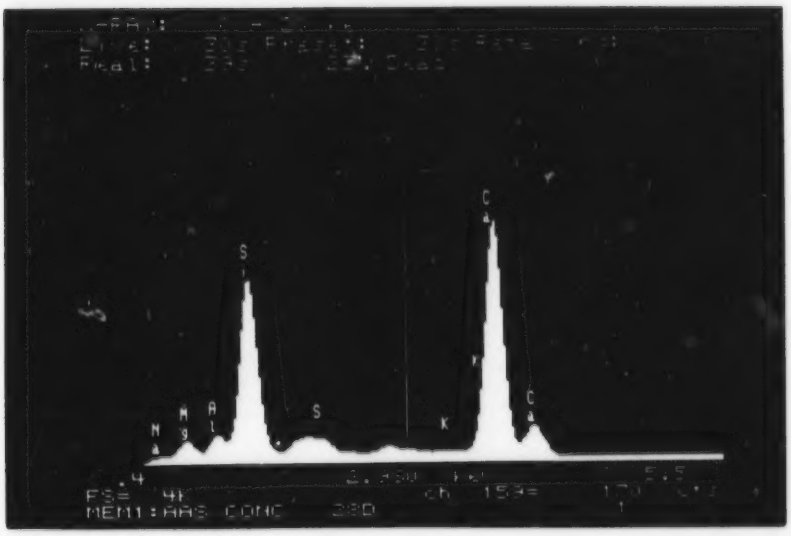

Fig. 30. Composition of gel in the same figure (Mg is lower)

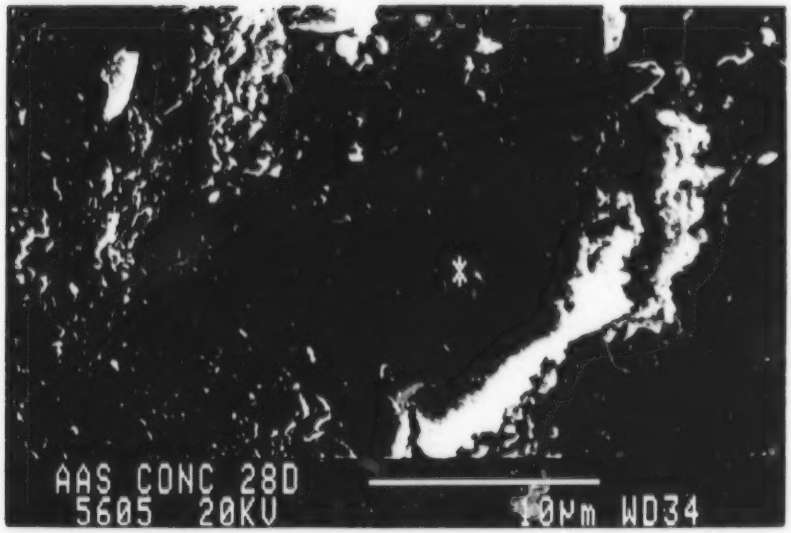

Fig. 31. A Na-rich zone in the paste

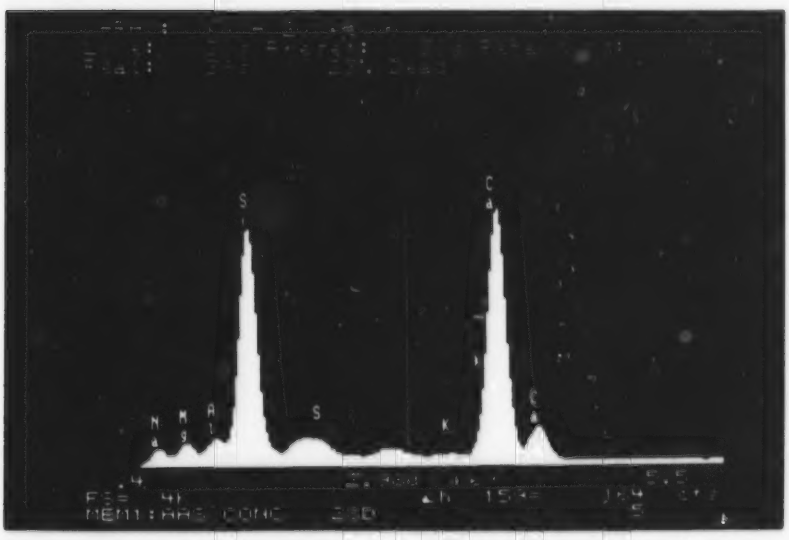

Fig. 32. Composition of this gel

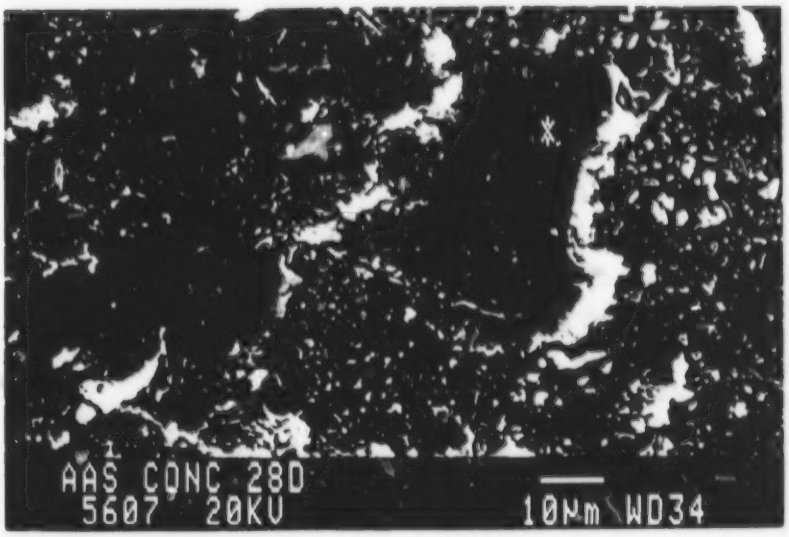

Fig. 33. The paste in the interfacial zone showing irregular masses

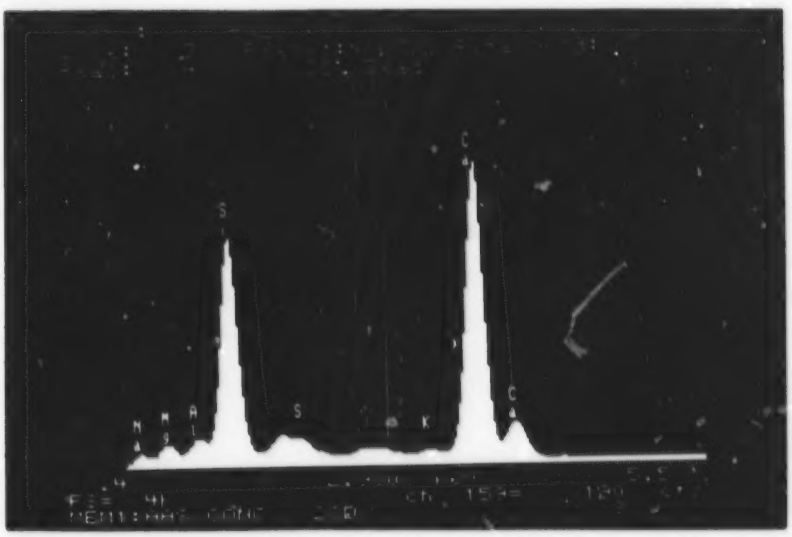

Fig. 34. The composition of the irregular mass, which is the same as the paste gel

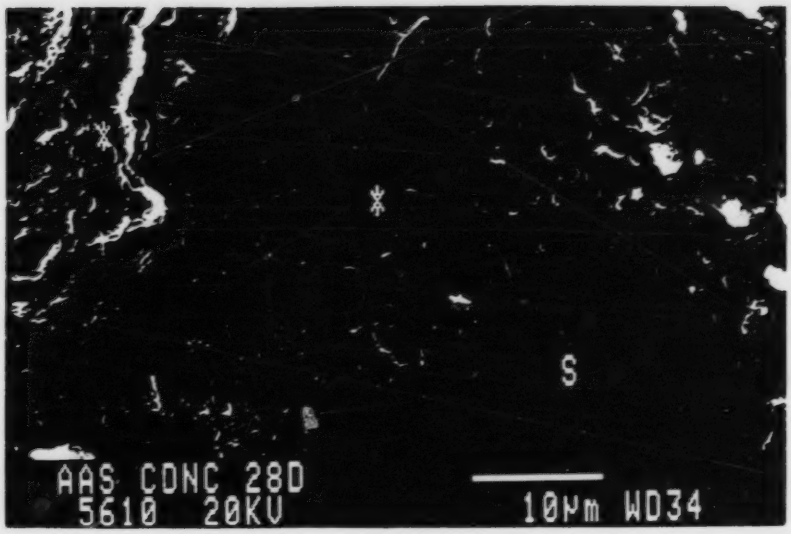

Fig. 35. A semipermeable membrane in the interfacial zone

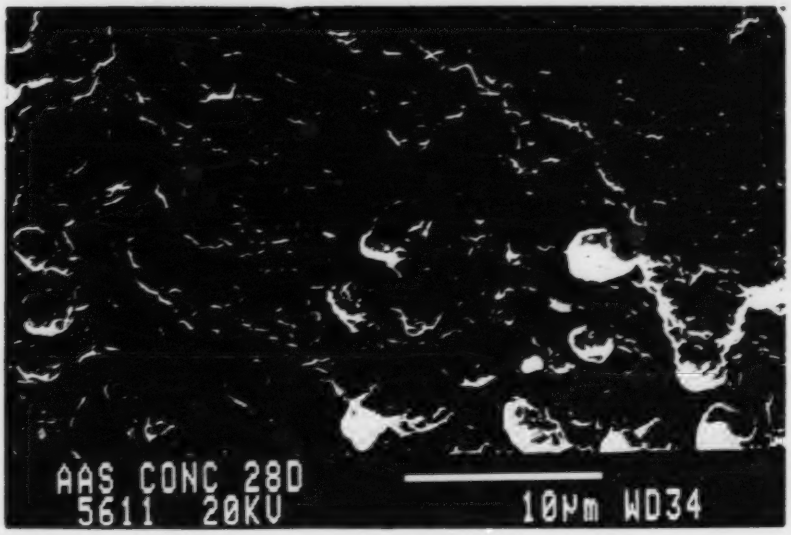

Fig. 36. Magnified view of this membrane showing the porous structure

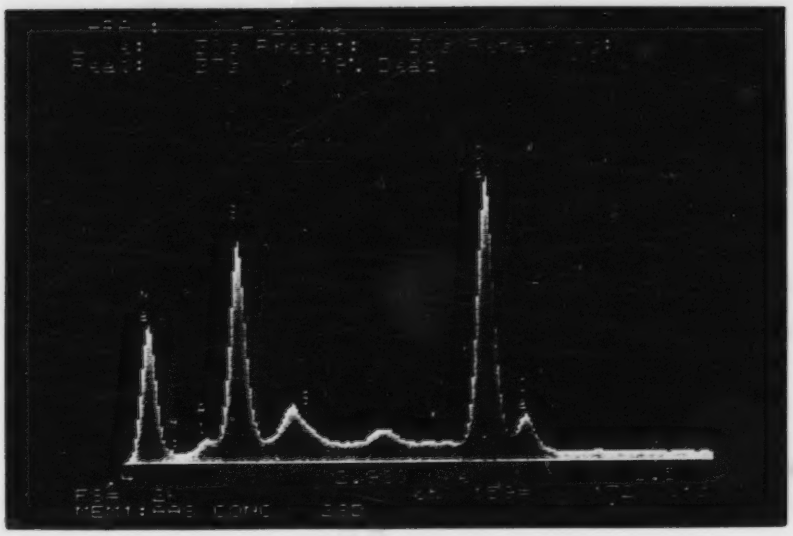

Fig. 37. Composition of this gel showing very high Na

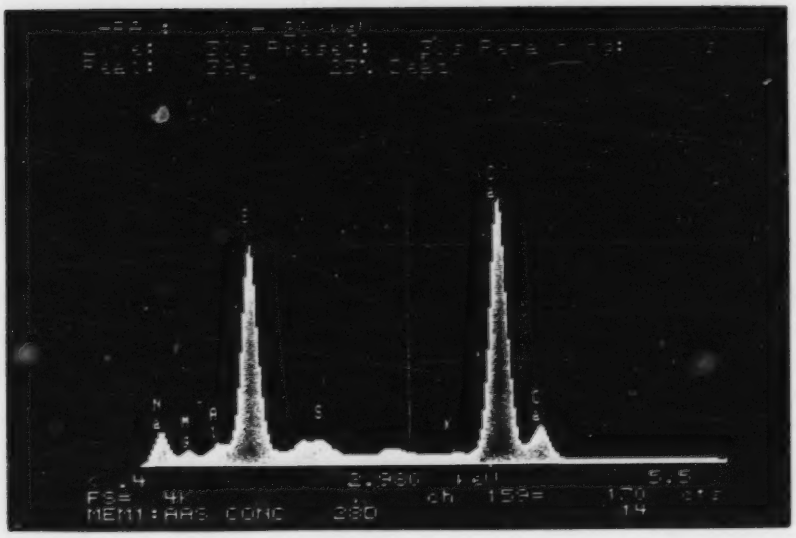

Fig. 38. Composition of this gel at another spot with much lower Na

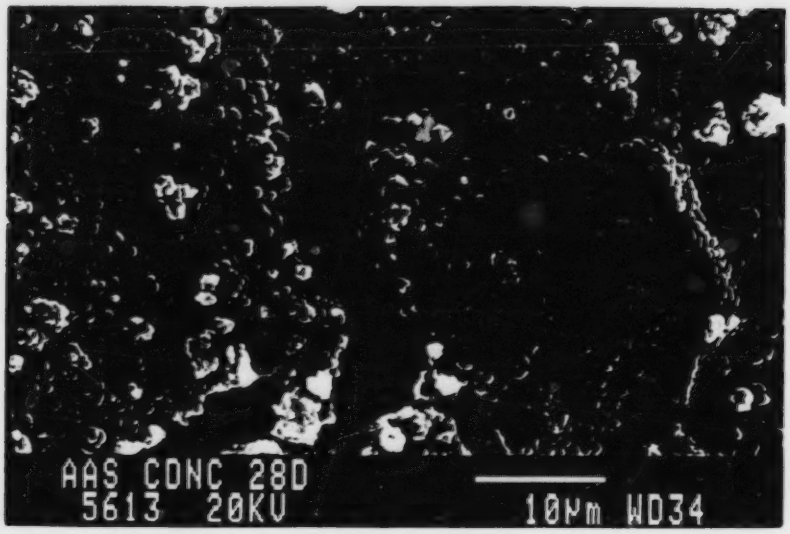

Fig. 39. Globular structure in the interfacial zone

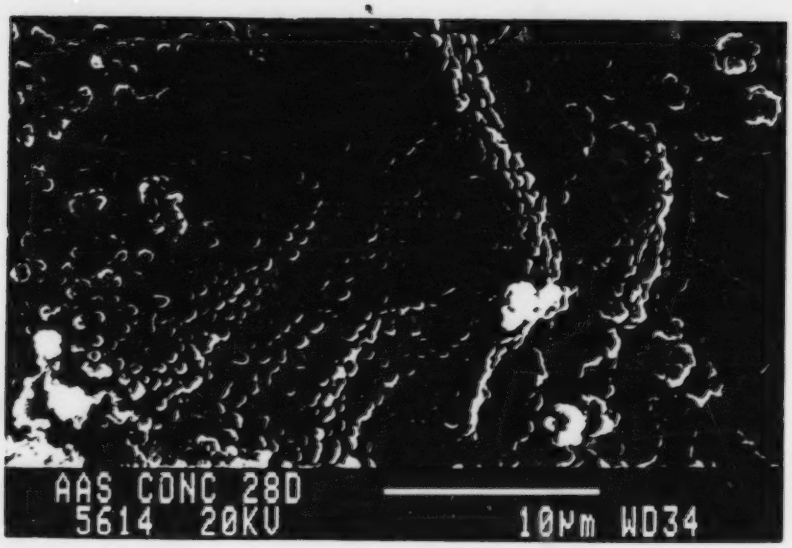

Fig. 40. Magnified view of this structure

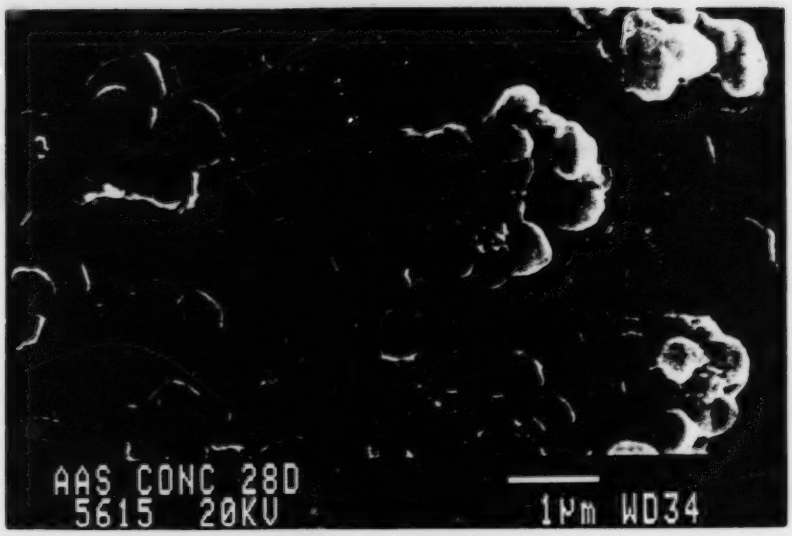

Fig. 41. Further magnification reveals the exact morphology of these globules

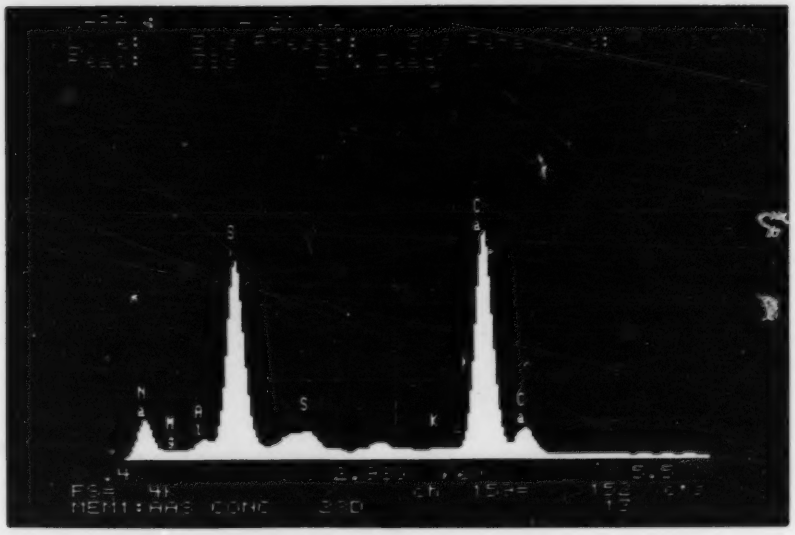

Fig. 42. Composition of an individual globule showing relatively high Na

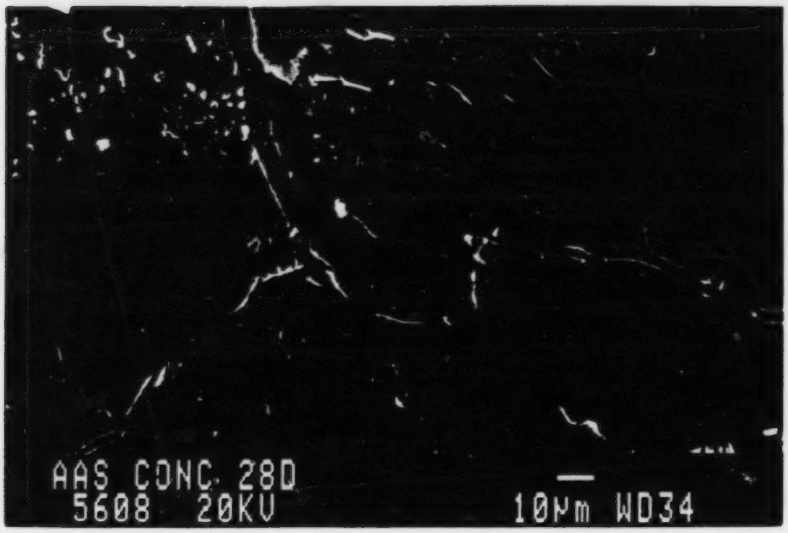

Fig. 43. Cracked gel in the paste

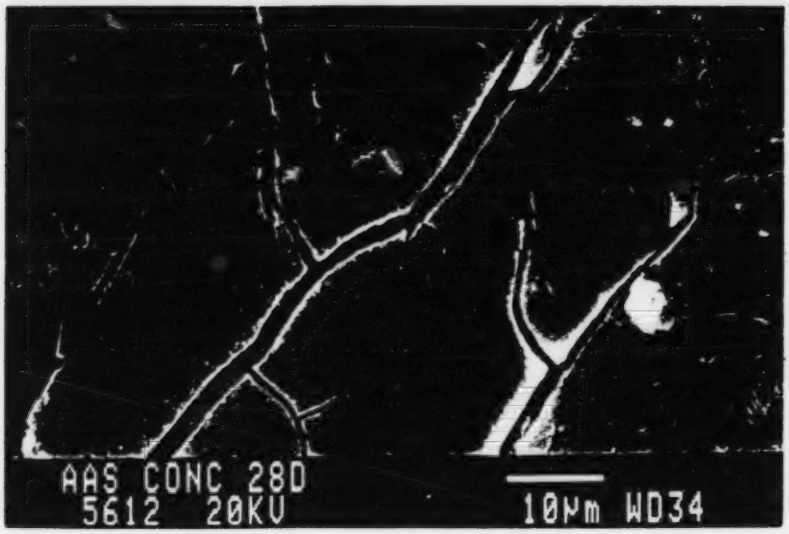

Fig. 44. Same feature at another location

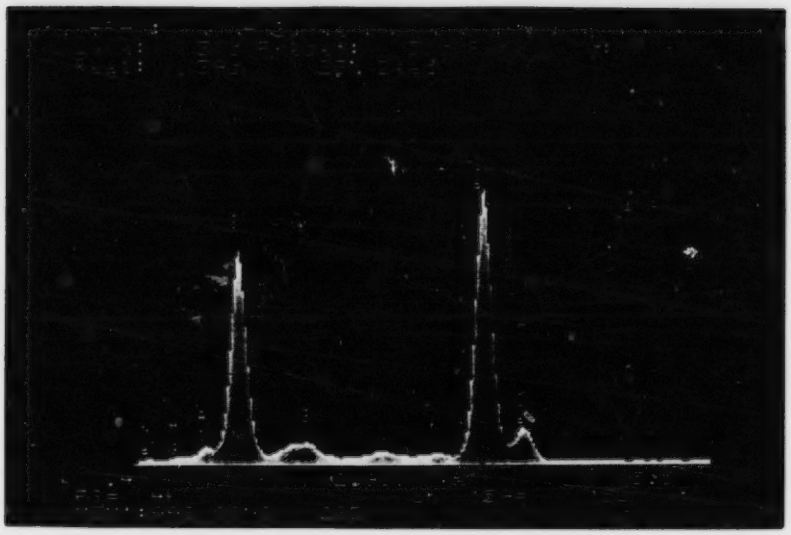

Fig. 45. Composition of this gel

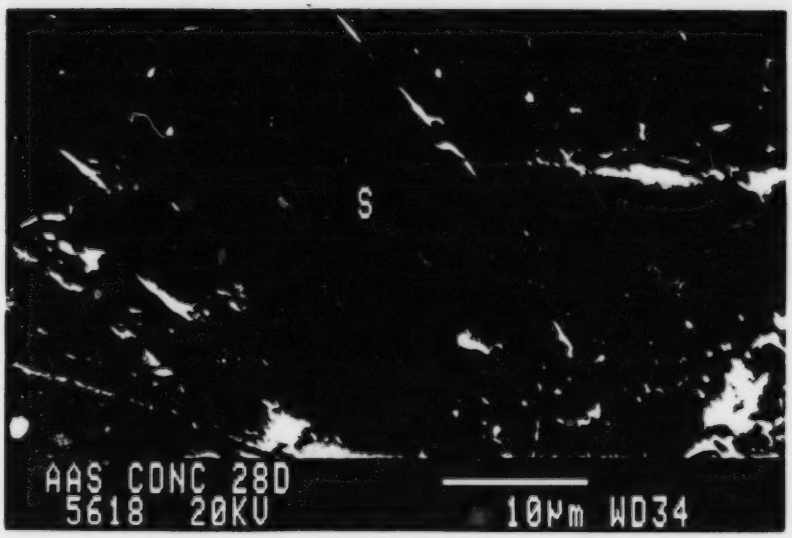

Fig. 46. A smooth intact grain of slag showing signs of peripheral reaction

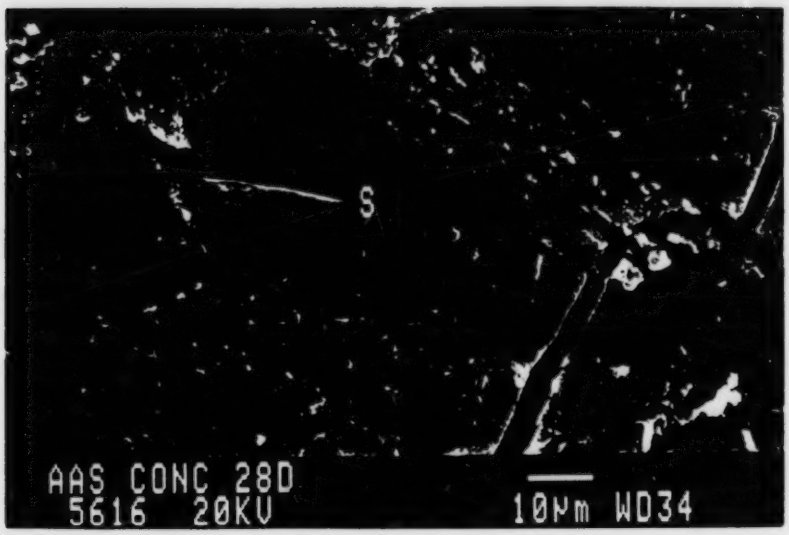

Fig. 47. A small slag grain with internal cracking

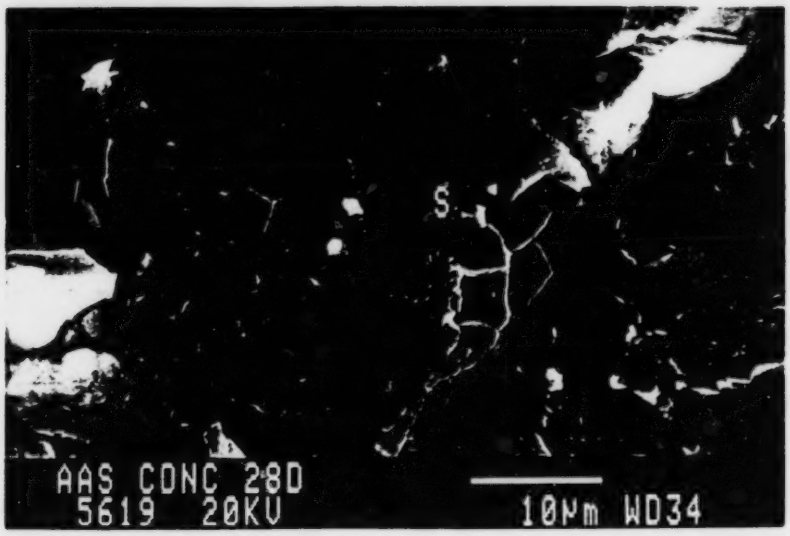

Fig. 48. A large slag grain showing the same type of cracking

Day 91: The strong paste-aggregate bonding whose development was observed at 28 days, continues without any sign of deterioration. This is shown in a series of micrographs (figs. 49-51). There is no change in the composition of the gel (with a small amount of Na) in the transition zone (fig. 52). Though the paste-aggregate bonding has developed, the gel in the transition zone nevertheless still exhibits ample cracking as can be seen in Figures 49-51.

The cracked gel in the paste is also present (fig. 53), and its composition has not changed (fig. 54). Some of this gel is composed of slag (fig. 55). In general, the paste is quite dense, except for the cracks, though there appears to some reduction in the width of these cracks, probably attributable to the healing effect due to hydration of slag. This, however, needs to be confirmed from porosimetry studies.

Smooth uncracked slag grains are as common in the paste (fig. 56), as ruptured grains (fig. 57), and grains with internal cracking (fig. 58). Peripheral reaction of smooth grains becomes vivid at this stage (fig. 59).

Microstructure of AAS concrete at 91 days

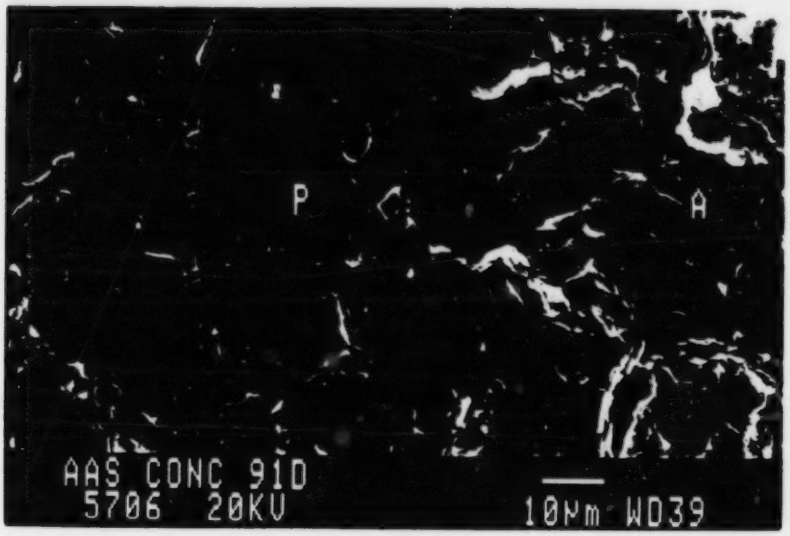

Fig. 49. Strong paste-aggregate bonding A- aggregate, P- paste

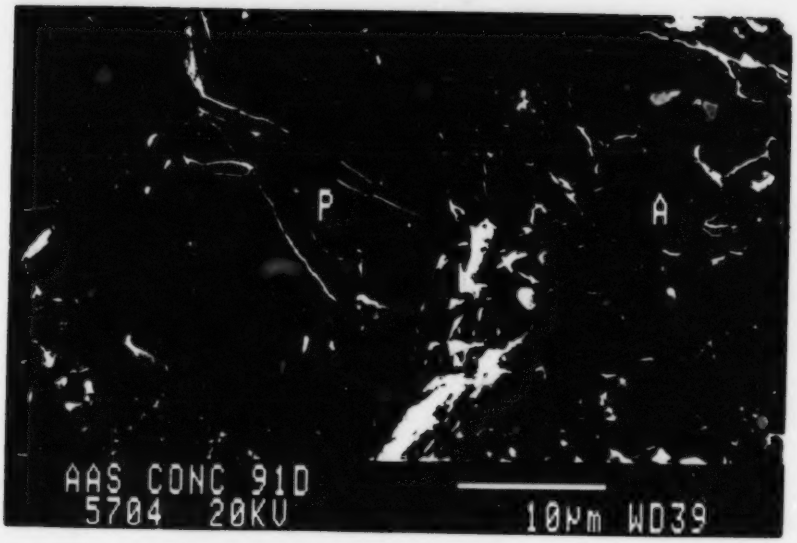

Fig. 50. Same feature at another place

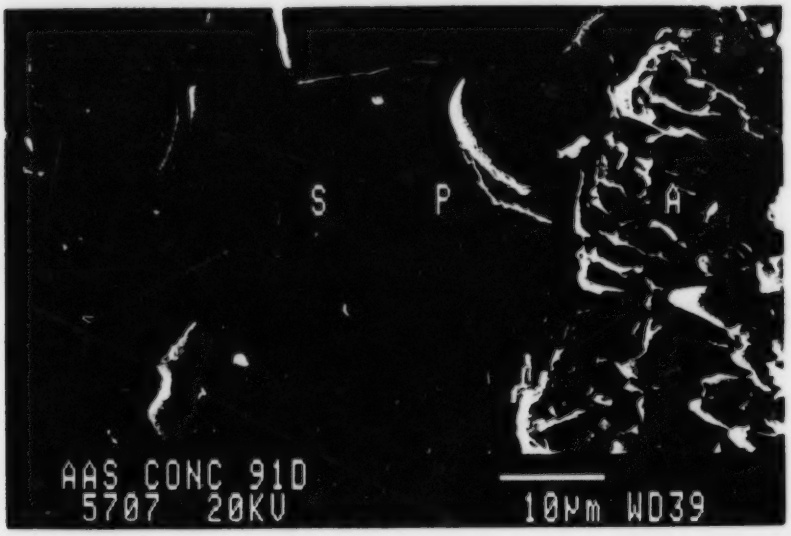

Fig. 51. Same feature. A small cracked slag grain (S) is visible

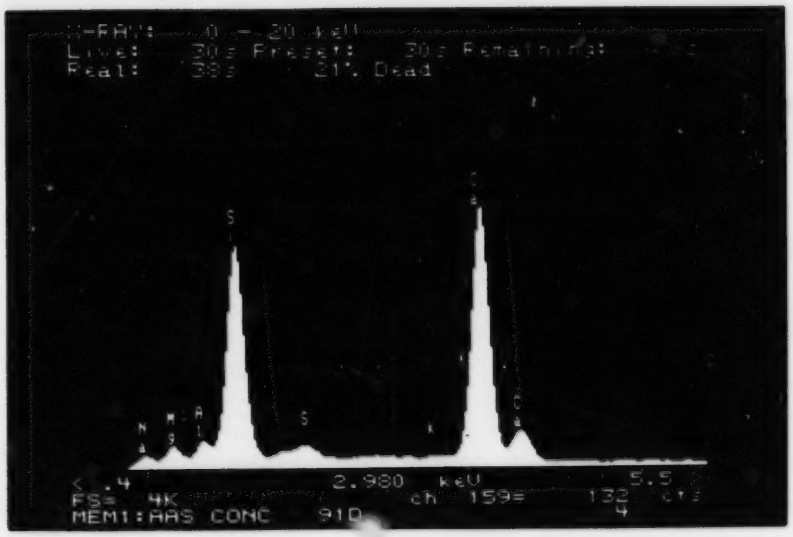

Fig. 52. Composition of the gel in the transition zone

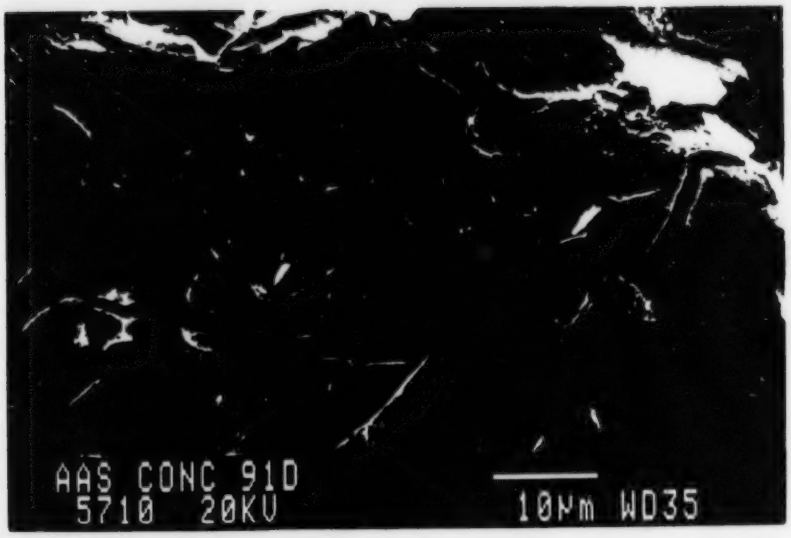

Fig. 53. Cracked gel in the paste

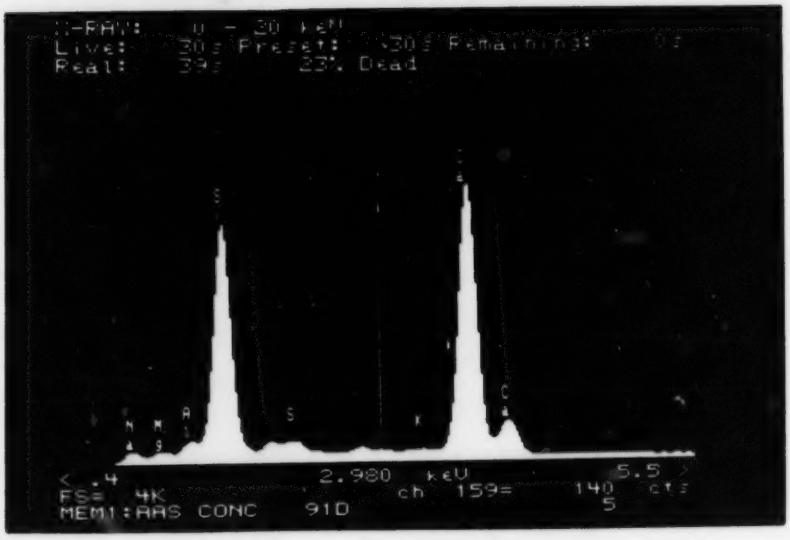

Fig. 54. Composition of this gel

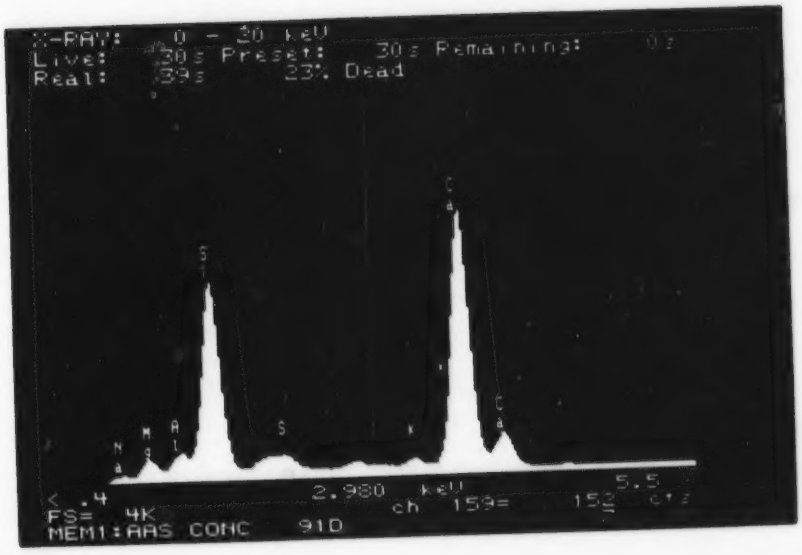

Fig. 55. Composition of slag in the paste

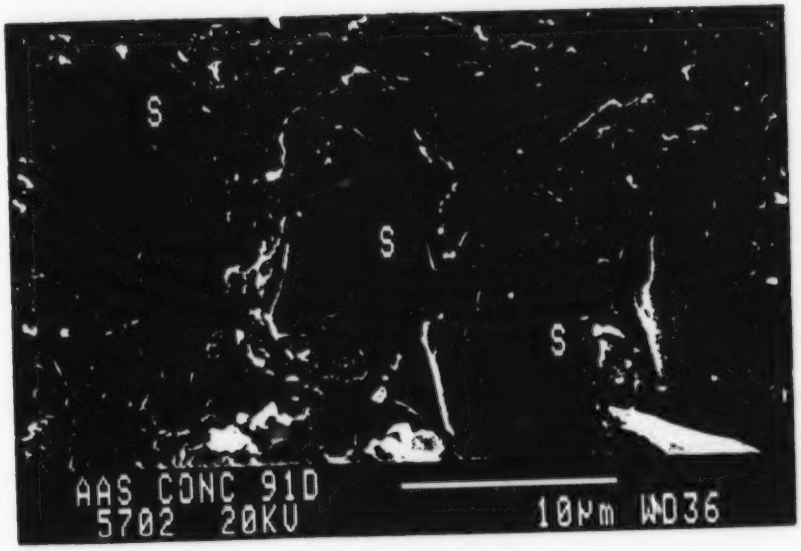

Fig. 56. Smooth intact slag grains in the paste

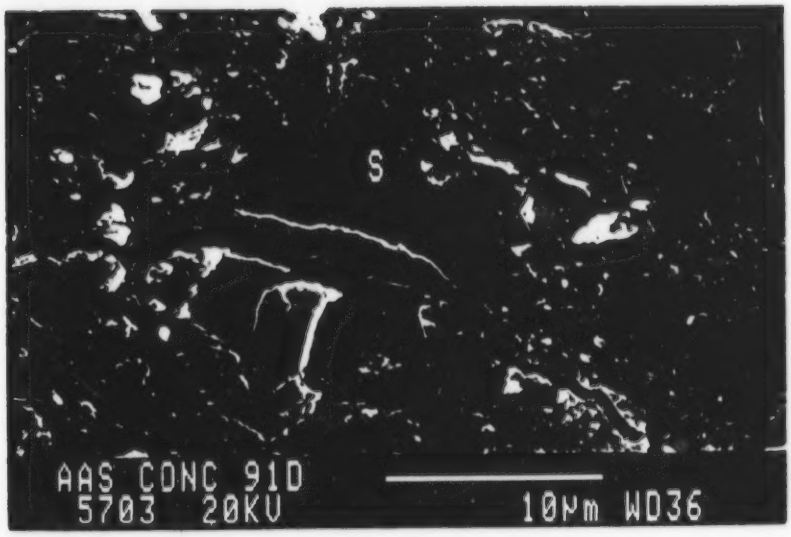

Fig. 57. A smooth but ruptured slag grain

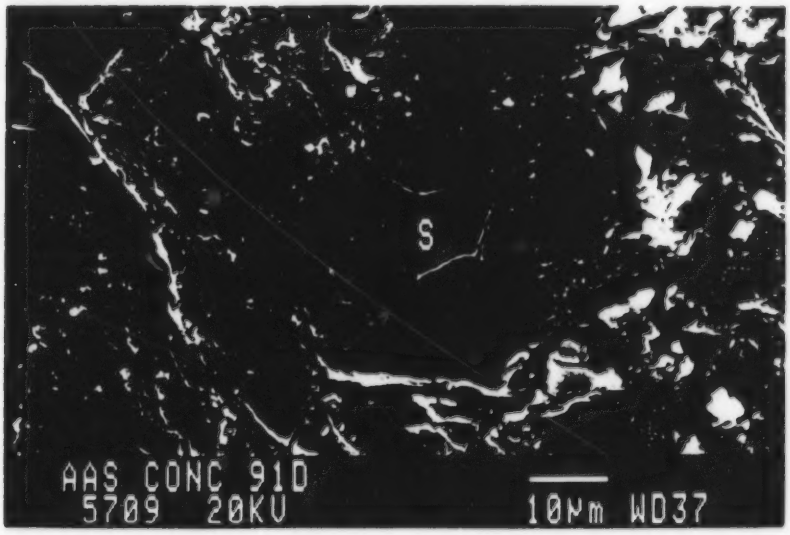

Fig. 58. Slag grain with internal cracking

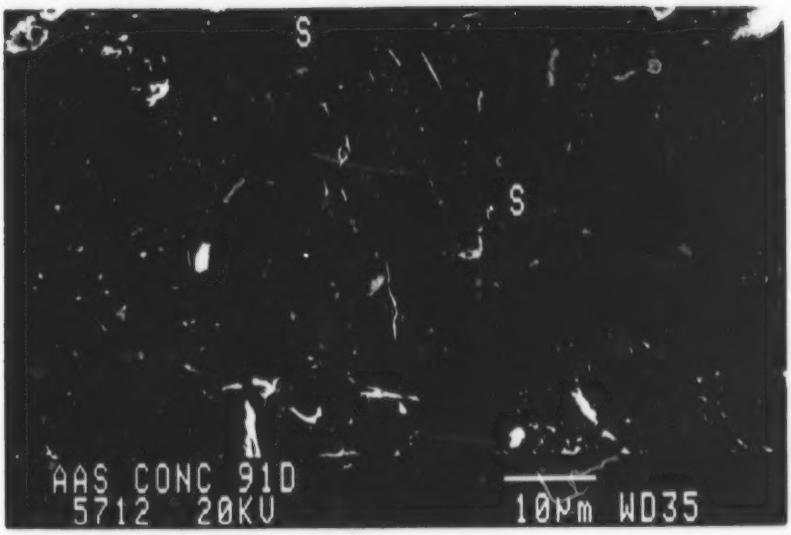

Fig. 59. Smooth slag grains showing peripheral reaction

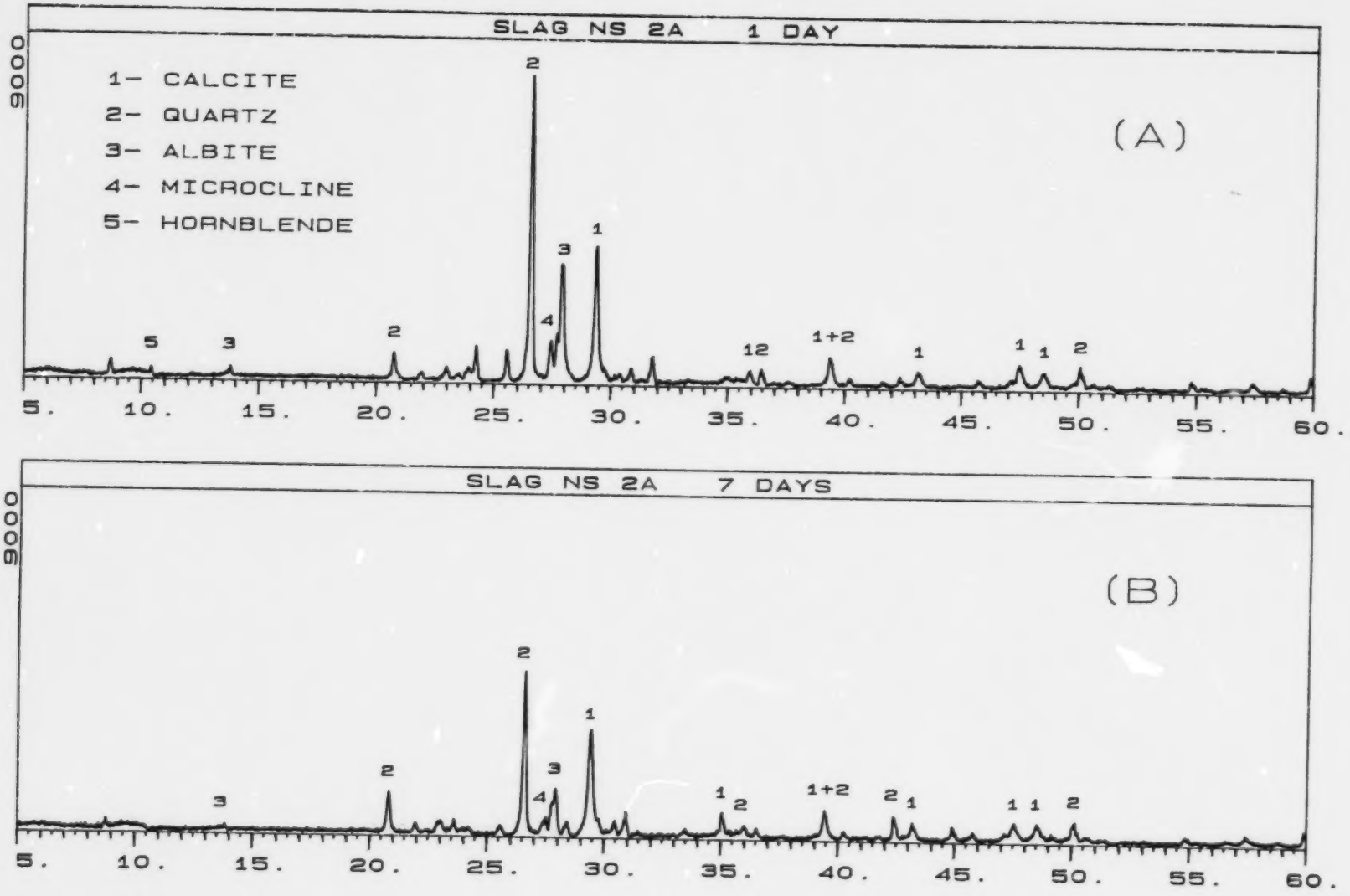
SLAG NS 2A 1 DAY
9000
1- CALCITE
2- QUARTZ
3- ALBITE
4- MICROCLINE
5- HORNBLENDE
(A)
5 3 2 4 3 2 1 12 1+2 1 1 1 2
5. 10. 15. 20. 25. 30. 35. 40. 45. 50. 55. 60.
SLAG NS 2A 7 DAYS
9000
(B)
3 2 4 3 2 1 1 2 1+2 2 1 1 1 2
5. 10. 15. 20. 25. 30. 35. 40. 45. 50. 55. 60.

FIG 60

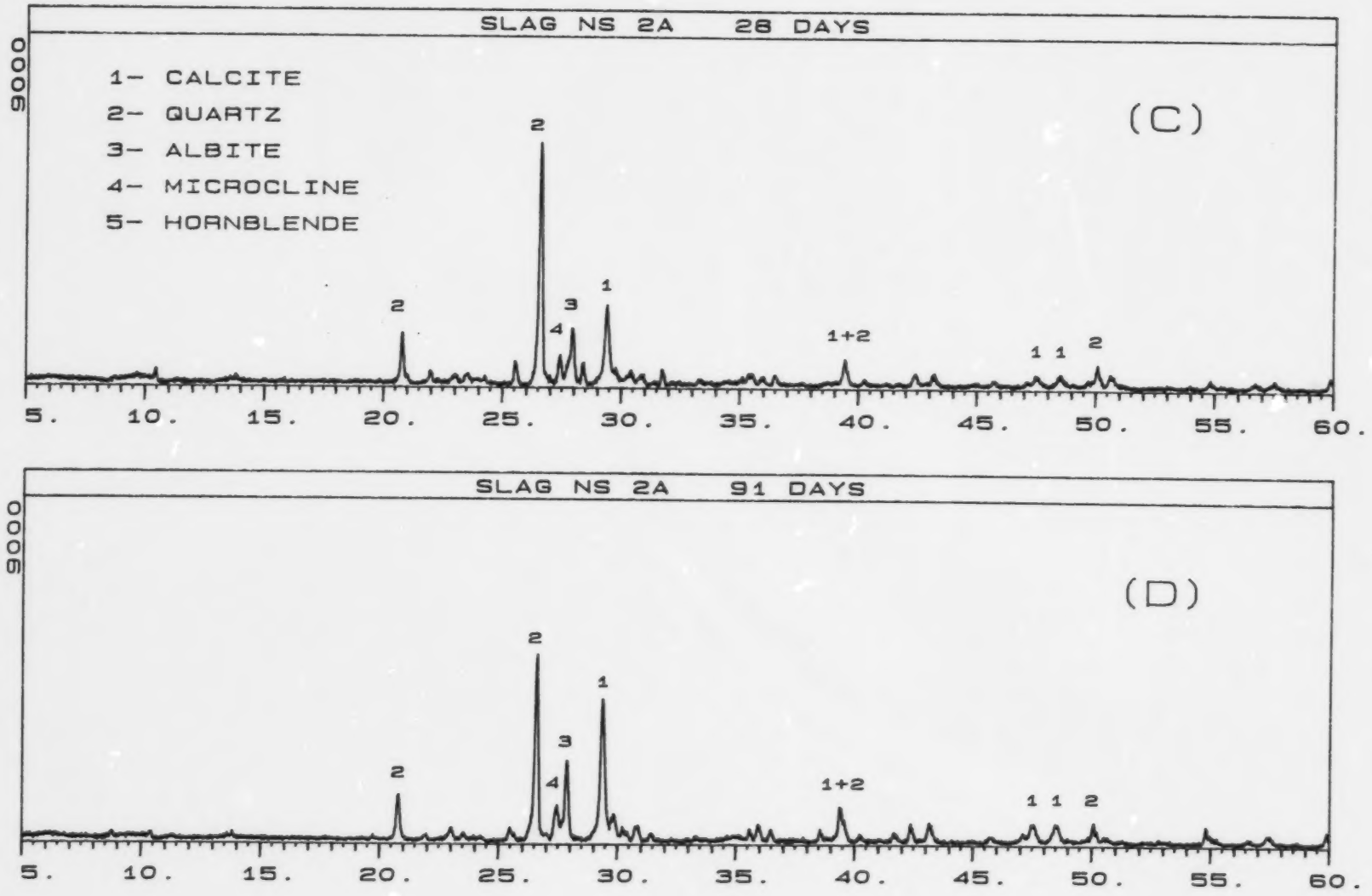
SLAG NS 2A 28 DAYS
9000
1- CALCITE
2- QUARTZ
3- ALBITE
4- MICROCLINE
5- HORNBLENDE
(C)
2
2
3
4
1
1+2
1 1
2
5. 10. 15. 20. 25. 30. 35. 40. 45. 50. 55. 60.
SLAG NS 2A 91 DAYS
9000
(D)
2
2
3
4
1
1+2
1 1
2
5. 10. 15. 20. 25. 30. 35. 40. 45. 50. 55. 60.

FIG 61

Summary of microstructural development

The paste-aggregate bonding does not develop cohesion until 28 days. At 1 and 7 days there are distinct signs of debonding in the transition zone. At 28 days, however, the paste-aggregate bond exhibits dramatic improvement, which continues up to 91 days.

The gel in the paste, though very dense, shows innumerable cracks at all stages of hydration right up to Day 91. The composition of this gel closely resembles C-S-H, except that the Ca/Si ratio is much lower. Small incorporation of Na, Mg and Al is noticeable, with occasional increase in Mg content, representing slag hydration. No significant change in composition of this gel is observed from 1 to 91 days, except for slight variation in Ca/Si ratio, though this variation is independent of the age. It appears to change with change in the composition of individual slag particles.

Slag with smooth surface becomes visible from the first day. This represents considerable departure from the morphology of normal slag hydration, which characteristically develops accicular structures on the surface of slag grains.

Slag grains begin to show signs of internal cracking from 7 days, though parallel with these grains, smooth uncracked grains also persist. Peripheral reaction, rather than the typical surfacial reaction, becomes visible from Day 7. The size of the grain does not affect this cracking phenomenon. The peripheral reaction is also independent of the size of the grain. This would suggest that both these features are related either to the mineralogical or the chemical composition of the individual grains.

The interfacial zone at Day 28 exhibits completely different microstructure, which comprises a semipermeable Na enriched membrane. This membrane is partly constituted of Na-rich microscopic globules. The

presence of this membrane, however, was not detectable in any of the other samples, which suggests that this may have been a result of localized concentration of Na_2SiO_3 (water glass) solution in the transition zone. In general, the transition zone gel composition is identical to the paste gel, and exhibits as numerous cracks as the paste.

XRD Analysis

XRDA of AAS concretes (figs. 60 and 61) proved inconclusive. The peaks of aggregates dominate the XRD traces, which renders it most difficult to identify the hydrate constituents. In addition, slag being constituted mainly of amorphous material, the number of identifiable crystalline peaks are very limited. Moreover, the principal hydration product is "gel", without any characteristic peak/s. The normal region of interest (20°-35° 2θ) is crowded with important peaks of calcite, albite, microcline and quartz arising from the coarse and fine aggregates. Thus, no positive identification of the hydration products could be made in this region.

Discussion

The high compressive strength observed at Day 1 (Table 2) is primarily due to the formation of dense silica rich gel from the reaction of water glass with lime. There is clear microstructural evidence of this Si-rich densified gel.

The upsurge in strength recorded at 7 days is attributable to the commencement of slag reaction. In the previous report it was noted that drastic microstructural changes occur at the third day when active slag hydration begins, resulting in considerably more C-S-H formation. This is reflected in the increase in strength at 7 days in the AAS concrete. This

phenomenon could have been more clearly established had the 3d compressive strength been recorded. In the case of the AAS paste, this increase (in strength) became distinctly noticeable at 3 days.

It is interesting that though the paste-aggregate bonding shows significant improvement by 28 days, the compressive strength increases very slightly. This suggests that the refinement in paste-aggregate bonding at 28 days is either not sufficient to warrant a corresponding increase in mechanical strength, or it only affects the flexural strength. Since only the flexural strength at 14 days (6.8 MPa) is available, no comments can be made at this stage on the influence of paste-aggregate bonding on the flexural strength, or whether it exerts significantly greater influence on the flexural strength than the compressive strength. According to Mehta (1) the presence of inhomogeneities is a very important factor which controls the tensile strength.

The chloride ion permeability results given below in Table 3 suggest that densification of the gel continues beyond 28 days. The non-negligible rise in compressive strength also points towards this direction. This obviously is due to continued reaction of slag, generating more C-S-H in the paste, which also appears to have a healing effect on the gel cracks leading to reduction in the permeability of the concrete. This healing effect, however, could not be precisely determined from SEM/EDXA; the gel appears to be cracked at all stages of hydration, beginning from Day 1.

TABLE 3

Chloride ion permeability (Coulombs) of AAS concrete

28d	91d
2547	1831

Thus, the microstructural development in AAS concrete (as in the AAS paste) can broadly be divided into two sections. The first phase represents the action of water glass, which occurs fairly early giving rise to a dense Si-rich gel and high strength. The second, which occurs at a later stage consists of continued hydration of slag. The cracks in the gel do not appear to affect the compressive strength which is reasonably high in this concrete, but is likely to affect the tensile strength. Tensile failure can occur by rapid propagation of a single microcrack, whereas a number of cracks must coalesce together to cause compressive failure, ie., much more energy is required to trigger a failure under compression (1). The paste-aggregate bond improvement probably helps in improving the tensile strength, rather than the compressive strength.

The gel cracks may be a cause for concern as far as durability is concerned, but the internal cracking of slag grains may be beneficial in the sense that this would allow the reaction to proceed much more rapidly. This in turn will lead to the formation of more gel,that could have a healing effect on the cracks.

Recommendations

(i) Flexural strength at different ages should be measured to determine the influence of gel cracks and paste-aggregate bonding.

(ii) Compressive and flexural strength at 3 days should be recorded to positively identify the beginning of slag hydration.

(iii) Mercury porosimetry studies at different stages of hydration should be conducted on paste samples to study the development and distribution pattern of macro and micropores with progressive hydration.